

Studies on DNA Interaction of Alanine and L-cysteine Functionalized ZnO Nanoparticles

Natarajan Prabakaran^{1,2*}, Chandrahasan Balamurugan², Sepperumal Murugesan³

¹Department of Chemistry, Yadava College (Autonomous), Madurai-625014, Tamilnadu, India.

²Bio-materials Research Division, Department of Chemistry, NPR College of Engineering and Technology, Natham, Dindigul-624401, Tamilnadu, India.

³Department of Inorganic Chemistry, School of Chemistry, Madurai Kamaraj University, Madurai-625021, Tamilnadu, India.

Abstract:- We have efficaciously stated the bioactive zinc oxide nanoparticles (ZnO NPs) in presence and absence of cetyl trimethyl ammonium bromide (CTAB) with the help of sodium hydroxide (NaOH). The prepared ZnO NPs were functionalized alanine and L-cysteine were characterized using UV-vis and FT-IR spectroscopic technique. The functionalized NPs were interact with DNA, it finds the groove binding.

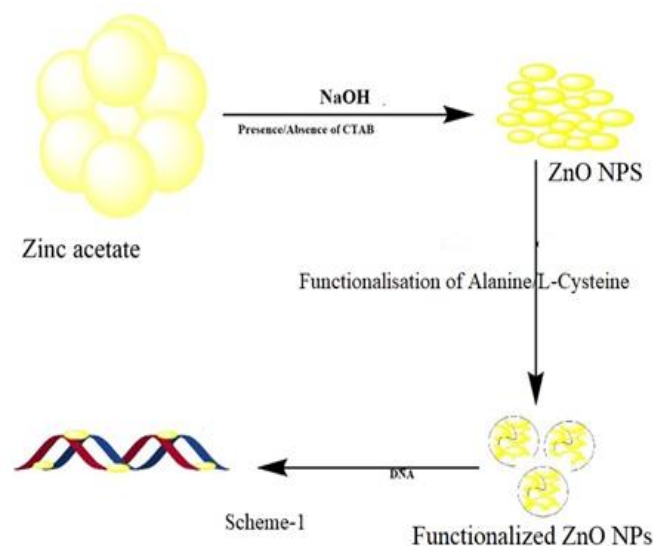
Keywords:- ZnO nanoparticles, aminoacid functionalised ZnO nanoparticles, DNA, groove binding, alanine-ZnO NPs, L-cysteine ZnO NPs.

I. INTRODUCTION

Over the last few decades, nanotechnology has witnessed an incredible development in the fastest-growing domain of science and technology because metal oxide nanoparticles (NPs) are progressively being used in bids of many industrials. Among the different metals, zinc attracts more attention because of its strong reducing potential, moderate reactivity, and having five stable isotopes. In the midst of the different zinc-based nanostructures like sulfide, ferrite, phosphide, selenide, and telluride, zinc oxide (ZnO) is most attractive due to its vast applicability, being eco-friendly, and its diverse physiochemical properties [1].

ZnO have a photo active compound, which influences the catalytic and oxidizing on chemical and biological species, respectively [2–4]. ZnO NPs, is a bio-safe material is compared to bulk ZnO. Actually, various studies have already revealed the potential toxicity of ZnO NPs based on their size, shape, and concentration, etc. [5, 6]. The U.S. FDA (Food and Drug Administration) granting ZnO has been permitted for use of cosmetic, the detailed toxicological profile and the mechanism of cytotoxicity for ZnO nanomaterials is, thus far, not fully understood [7]. Moreover, ZnO NPs are testified to have a good biocompatibility with anthropological cells, and the ZnO has been documented as a safe material by the FDA [8, 9], although the intrinsic cytotoxicity of ZnO NPs against certain human cell lines has raised some apprehension concerning potential health hazards [10]. On the other hand, their inherent cytotoxicity indicates a necessary quality against pathogenic cells if the properties are precisely tailored [7, 11]. Indeed, recent studies have revealed that ZnO NPs have cytotoxic effects toward cancerous cells, while at the same concentration, ZnO NPs have negligible effects on normal

cells, leading to speculation that they can be used in cancer treatment. On the other hand, for more pervasive applicability in modified forms of ZnO NPs, for example, through appropriate polymeric materials with surface coatings [12–14] or green chemical approaches (capping with phytochemicals) and bio-inspired manufacturing [14–16] that might perfection their biocompatibility. In our group previously reported the metal and metal oxides nanoparticles such as nickel, copper and magnetic materials to interact with DNA to form the structural reformation of DNA with helpful of drug delivery [17–19]. Herein we discuss the spectral supported the DNA interaction studies of prepared and characterized ZnO NPs stabilized with or without CTAB and biomolecules of alanine and L-cysteine functionalized ZnO NPs (Scheme-1).



II. EXPERIMENTAL METHODS

A. Materials and Methods

All required chemicals were AR grade purchased from Himedia, Qualigens, Sdfine and Sisco chemicals chemicals Pvt. Ltd from India and were used as received. Zinc acetate dihydrate, sodium hydroxide, sodium chloride, Tris-HCl and L-cysteine (Merck), herring sperm DNA and cetyl trimethyl ammonium bromide (CTAB) (LOBA Chemie) and were used as received.

The prepared ZnO NPs as well as functionalized ZnO NPs were characterized using SEM-EDX (Hitachi S-3400, EMax Horiba analysis), XRD (Philips X^{pert}-MPD) and SCHIMADZU FT-IR 8400S (4000 – 400 cm⁻¹) spectrophotometer were corroborate the functional group modification. The DNA binding studies were characterised using UV-vis (Jasco-550), electro chemical analyzer (BAS CV-50W), circular dichroic spectra (Jasco J-810) and viscosity of DNA interactions (BROOKFIELD DV-II+PRO) in this method.

B. Synthesis of ZnO nanoparticles (ZnO NPs) and alanine , L-cysteine functionalized nanoparticles.

➤ **Preparation-1**

We prepared the ZnO nanoparticles in Wang [20] modified procedure. The aqueous solution containing 1.1 g (5 mmol) zinc acetate dihydrate and 0.4g (10 mmol) NaOH was prepared. The addition of sodium hydroxide in dropwise to the precursor of zinc acetate dihydrate under stirring. The total volume of the reaction mixture was made up to approximately 250 mL by adjusting the water volume. While adding NaOH solution a white milky solution was formed. After all the NaOH was added, the stirring was continued for next half an hr. Then the mixture was refluxed for 4 hrs at 100 °C. After completion of refluxing, the resultant product reaction mixture was cooled to room temperature and separated the ZnO NPs centrifuged at 10,000 rpm for 30 min. The ZnO NPs was washed, dried, stored and used for further studies.

➤ **Preparation-2**

5 mmol of (1.1 g) zinc acetate dihydrate in water and 0.3644 g (1 mmol) of CTAB in water were mixed and stirred for 3 hrs. Then, 0.4 g (10 mmol) of NaOH into the above mixture under stirring in dropwise. The total volume of the reaction mixture was made up to approximately 250 mL. A milky white color solution was formed and stirring was continued for next 1 h. Then, the reaction mixture was concentrated for 2 h to room temperature, it was standby and diluted. The prepared ZnO NPS was centrifuged for 30 min at 10,000 rpm and washed with water. Finally, the settled ZnO was dried and collected as white powders.

➤ **Preparation-3**

30 mg of ZnO NPs which was prepared by the procedure described in preparation 1 and 0.1756 g of L-Cysteine hydrochloride were dissolved in 40 mL water and the reaction mixture was refluxed for 10 hrs. Then, the reaction mixture was allowed to standby overnight. After, the mixture was sonicated for 1 h and the mixture was evaporated to dryness in air. The resulted L-Cysteine functionalized ZnO NPs was stored.

➤ **Preparation-4**

30 mg of ZnO NPs were dispersed in 10 mL of water and then added with 1 mmol of L-Alanine made upto 50 mL using double distilled water, the reflexion of reaction mixture for 10 hrs. Then, the reaction mixture was allowed to standby overnight. After, the mixture was sonicated for 1 h and the functionalized mixture was evaporated to dryness in air. The

resulted L-Alanine functionalized ZnO NPs was collected and stored.

III. RESULTS AND DISCUSSION

A. SEM and XRD studies

Figure 1 shows the SEM image and energy dispersive spectra (EDS) of the ZnO NPs. From this data reveal that the observed particles size range of 60-70 nm. EDS analysis also exhibits the presence of Zn, Ca, and O, confirming that the particles are ZnO nanoparticles (data are present in the figure). Fig. 1b and 1c are the magnified SEM images of ZnO nanoparticles prepared in water dispersion.

To further confirm the formation of ZnO nanoparticles and its crystallinity, XRD pattern were recorded. Figures 2a and 2b show the XRD patterns of the ZnO and cysteine functionalized ZnO. In figure 2 the Braggs peaks observed at 2θ 31.86°, 34.48°, 47.6°, 56.62°, 63.0°, 68.0° and 69.16° shows the presence of hexagonal ZnO (wurtzite). (JCPDS No. 36-1451) which are fitting in to the crystal plane (1 0 0), (0 0 2), (1 0 1), (1 0 2), (1 1 0), (1 0 3), (1 1 2) and (2 0 1) respectively. The relatively broad peak observed in the XRD reveal that the ZnO particles are <100 nm. The results of XRD and EDS indicate that we can prepare the ZnO similar to wurtzite phase [21-23]. The average size assessed from the major diffraction curve, using the distinguished Debye-Scherrer's formula (Eq. (1)):

$$D = 0.94 \lambda / B \cos\theta \dots\dots\dots (1)$$

where λ is the wavelength, B the full-width at half maximum of the peak in radians and θ the Bragg's angle of the XRD peak was found to be about 60 nm for ZnO NPs and ZnO was 80 nm for cysteine functionalized ZnO due to formation of strong complexation.

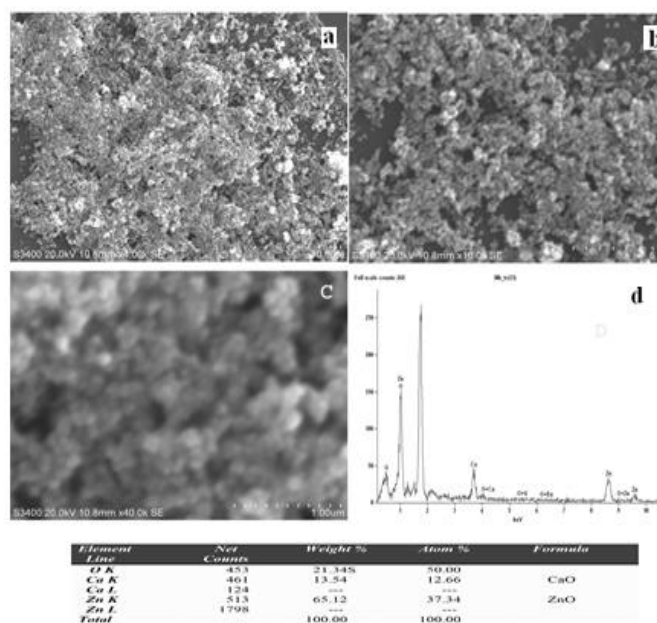


Fig 1:- ZnO NPs of low intensification (a), high magnification (b&c) of SEM and EDS (d).

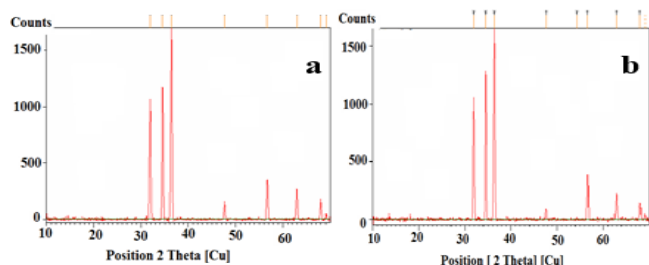


Fig 2:- Powder XRD pattern of the (a) ZnO NPs and (b) cysteine functionalized ZnO NPs

B. UV-Vis spectral studies

The fascination of ZnO NPs were studied using electronic spectra, which were prepared without stabilizing agents, dispersed in various solvent medium such as acetone, ethanol and water were shown in figure 3. The absorption of ZnO NPs observed around 360 to 374 nm and varying absorption strength due to dispersion rate. We have chosen hydrophilic solvent water for further application studies. Further, we interested to functionalize the ZnO NPs using amino acid such as cysteine and alanine. Figure 4 expressions the UV-vis absorption spectra of amino acid functionalized ZnO NPs. In alanine and cysteine functionalized ZnO NPS observed the weak absorption at 372 nm, which shows the confirmation that ZnO NPs are functionalized with amino acids [24].

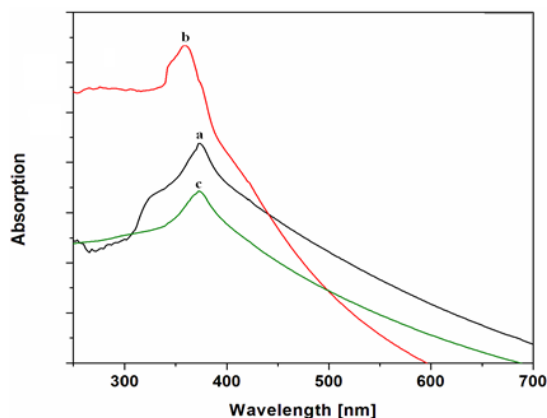


Fig 3:- UV-vis spectra of ZnO NPs dispersed in various solvent (a) water, (b) ethanol and (c) acetone

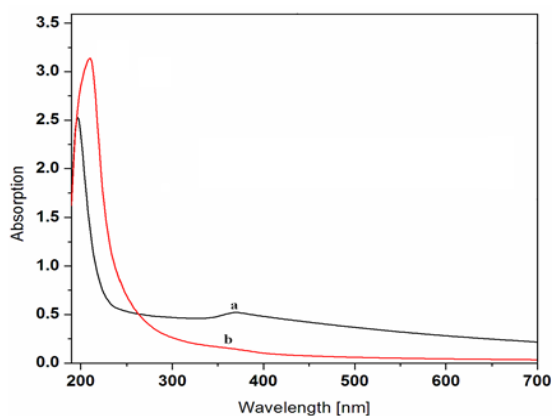


Fig 4:- UV-vis spectra of (a) alanine functionalized ZnO NPs (b) cysteine functionalized ZnO NPs in water

C. FT-IR spectral studies

FT-IR spectra recorded for the bare ZnO NPs and with cysteine/alanine functionalized ZnO NPs are shown in Fig 5. The FTIR spectrum of bulk ZnO showed a high intensity broad band around 460 cm⁻¹ due to the stretching mode of the zinc and oxygen bond, which is similar in nano-ZnO [25]. The FTIR spectrum of ZnO NPs prepared without CTAB shows a broad band at 450 cm⁻¹ which corresponds to ZnO and another broad wide band observed at around 3402 cm⁻¹ which may be due to the presence of hydroxyl groups, most likely present on the particle surface.

In Fig 5 b and c 2586 cm⁻¹ shows the vibrational band for -SH present in the cysteine capped ZnO nanoparticles which is present in the prominent -SH vibrational band observed in 2561 cm⁻¹ is organic moiety of amino acid. The N-H stretch of cysteine molecule is observed at 3377cm⁻¹ but, upon coordination with the ZnO surface, the peak red shifted to 3492 cm⁻¹. The relative transmittance were suggests interaction of the -NH₂ and -SH group with ZnO for the surface binding of cysteine and alanine with ZnO particles via -SH and -NH₂ linkage and approves well with prior reports on gold and silver nanoparticles [26, 27]. Further, we found the strong absorption around at 1632 cm⁻¹ is present in the carboxylate [1620 cm⁻¹] stretching of the cysteine and alanine molecule in ZnO NPs. Therefore, the shift is present due to acetate ion in carboxylate functionality.

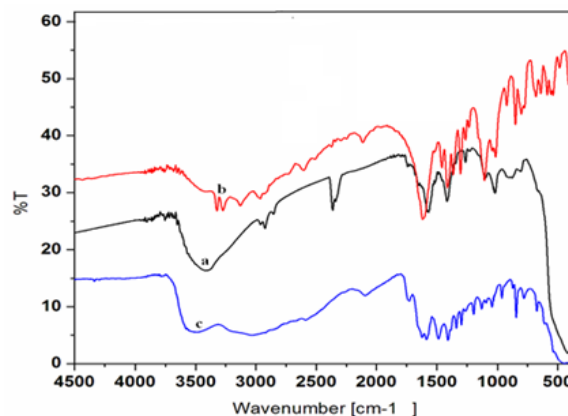
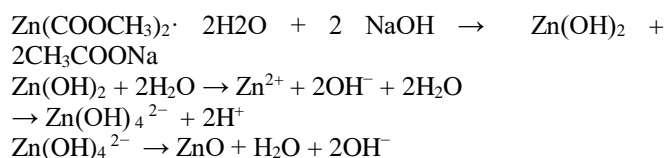


Fig 5:- FT-IR spectra of (a) ZnO NPs, (b) alanine functionalized ZnO NPs and (c) cysteine functionalized ZnO NPs.

Briefly, in the aqueous synthesis of ZnO nanoparticles, the initial precipitate of the reaction is Zn(OH)₂, which by subsequent modifications produces ZnO nanoparticles. The high repulsive forces between the lone pair of electrons of two oxygen atoms of zinc hydroxide facilitate the dehydration quite quickly at low temperature, resulting in the formation of ZnO nanoparticles. The possible chemical reaction is given below [24]:



D. DNA binding studies

➤ Electronic spectral studies

The ZnO and amino acid functionalized NPs were dispersed in water and then interacted with DNA. DNA has the characteristic absorption band at 260 nm. In order to find the mode of interactions of DNA with ZnO NPs, around 300 micro molar solution of DNA was titrated with increasing concentration of ZnO or functionalized ZnO NPs. On increasing DNA concentration, we observed hypochromic at 372 nm and hyperchromic at 260 nm (figure 6(i)) and slightly blue shifted on both. Further in the same way when functionalized NPs concentration were increased, the absorption bands showed hypochromic with slightly red shift of about 2 nm as shown in Fig. 6(ii) and (iii), additional the emergence of isobestic points between 218 and 242 nm. On the addition of functionalized NPs to DNA, considerable drops in the absorptivity of π to π^* bands of DNA solution were observed in all the systems.

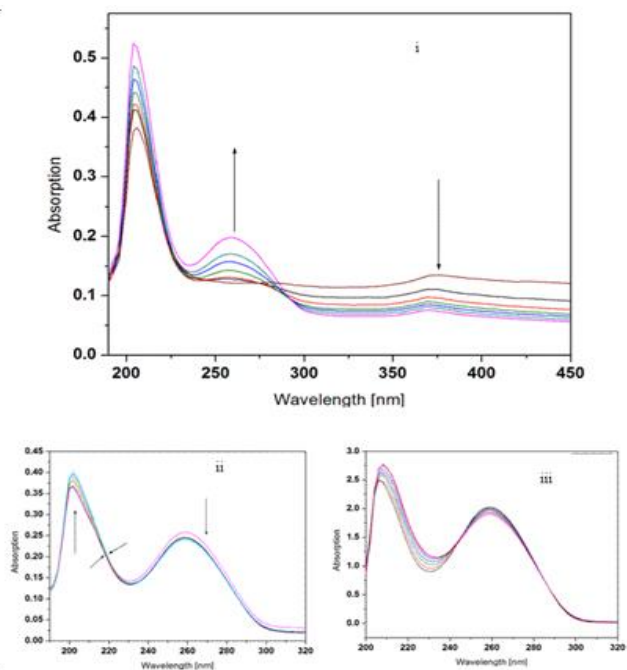


Fig 6:- UV-visible absorption spectra of (i) DNA with increasing amount of ZnO NPs, (ii) DNA with increasing amount of alanine functionalized ZnO NPs and (iii) DNA with increasing amount of cysteine functionalized ZnO NPs

The intrinsic binding constant K_b for the interaction of these nanoparticles with DNA has been calculated from the absorption spectral titration data.

$$[DNA] / (\epsilon_a - \epsilon_f) = [DNA] / (\epsilon_b - \epsilon_f) + 1 / K_b (\epsilon_b - \epsilon_f) \text{ -----(2)}$$

In the plot of $[DNA] / (\epsilon_a - \epsilon_f)$ vs $[DNA]$, K_b is given by ratio of the slope to intercept. Binding constant value is estimated as $1.307 \times 10^5 M^{-1}$. The amino acid functionalized nanoparticles also shown the same behaviors, the observed binding constant values are $2.531 \times 10^4 M^{-1}$ and $4.23 \times 10^4 M^{-1}$ for the ZnO nanoparticles prepared using alanine and cysteine respectively. The spectroscopic changes suggest that there are some interactions between the ZnO NPs or functionalized ZnO NPs and DNA. The K_b values are lower than the typical intercalators like ethidium bromide with 7 x

$10^7 M^{-1}$ in 40 mM Tris-HCl buffer, pH 7.1 having a proven DNA binding mode involving the complete insertion of the planar ethidium bromide molecules between the base pairs. The lower values indicate binding of nanoparticle with DNA host with an affinity less than the classical intercalator.

➤ Redox studies

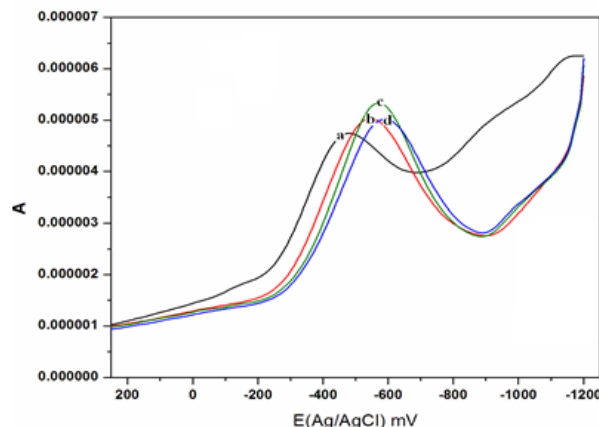


Fig 7:- Differential pulse voltammogram of ZnO NPs with increasing amount of DNA (R= 0.07 to 0.7; a = 0.07, b = 0.14, c = 0.28, d = 0.48 and e = 0.7) in buffer at 100 mV/s

Differential pulse voltammogram (DPV) experiments were performed to observe the shift in formal potential along with the current intensity on the addition of DNA to ZnO NPs or functionalized ZnO NPs in Tris buffer solution. The process was monitored as a function of added DNA with constant concentration of ZnO NPs or functionalized ZnO NPs (figure 7 and 8). On the addition of 300 μM DNA to ZnO NPs there is increase in the current intensity up to 100 μL with huge potential variation on both sides. On further addition there is decrease in the current intensity and move towards negative side. When the alanine functionalized NP solution was titrated with DNA, the current intensity increases initially and then decrease with the increasing DNA concentration while the potential were move towards negative side. The same behavior was followed in the cysteine functionalized NPs with DNA.

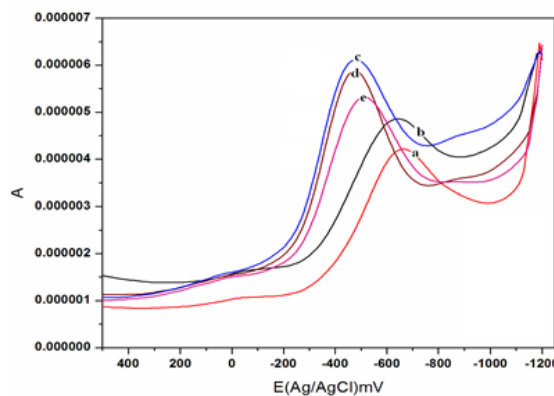


Fig 8:- Differential pulse voltammogram of alanine functionalized ZnO NPs with increasing amount of DNA (R= 0.01 to 0.1; a = 0.01, b = 0.03, c = 0.06 and d = 0.1) in buffer at 100 mV/s

➤ Circular Dichroism spectra

Circular dichroism (CD) of the perturbed DNA is one of the choicest methods to monitor the conformational changes brought about by the interacting host molecules. The UV-CD spectrum of DNA exhibits a positive absorption band at 275 nm due to the base stacking and a negative band at 245 nm due to the helicity of DNA. The conformational changes upon the addition of Zinc oxide nanoparticles was studied by keeping the concentration of DNA constant and varying the concentration of Zinc oxide nanoparticles in the ratio of 1/R values from 1 to 5 in a buffer solution (pH = 7.1) where $R=[\text{DNA}]/[\text{ZnO NPs}]$. The spectrum of the control DNA and with the additives was monitored from 220 to 320 nm. Figure 9 shows the induced structural changes of DNA by the addition of Zinc oxide nanoparticles in the terms of the ellipticity. It is a known chemistry that, the changes in ellipticity are directly related to the conformational changes observed from the circular dichroism. The small changes in the positive and negative peak were observed for the addition of nanoparticles solution to DNA. This indicates the interaction between the nanoparticles and DNA induces only slight modifications at the native conformation of DNA. This phenomenon could be due to the groove binding of the nanoparticles possibly stabilizes the right-handed B form of DNA through H-bonding with phosphate back-bone. Earlier, Frenc et al. reported that the minor groove binding through the partial intercalator is non-degenerate excitation interaction [28]. All the ZnO nanoparticles are bind with DNA through the minor grooves.

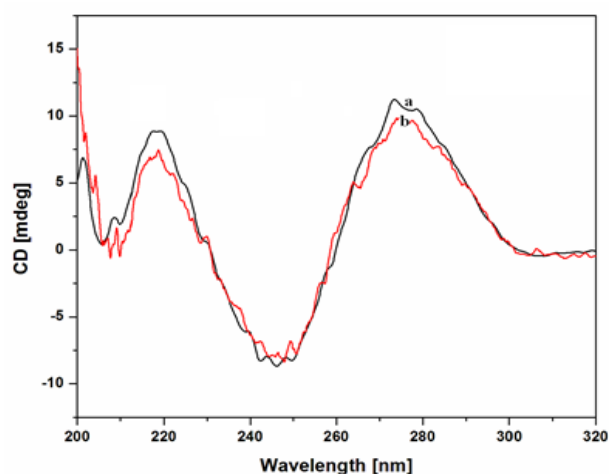


Fig 9:- UV-CD spectra of DNA with of ZnO NPs (1/R= 0 to 5: a= 0 and b= 5).

➤ Viscometric studies

Viscosity measurements were carried out on herring sperm DNA by varying the concentration of ZnO nanoparticle. It has already been proved that, under appropriate conditions intercalation of molecules like ethidium bromide (EthBr) causes a significant increase in viscosity of DNA solutions due to increase in separation of base pairs at intercalation sites and hence an increase in overall DNA contour length. In contrast, drug molecules that binds exclusively in the grooves of DNA, under the same conditions, causes less pronounced or no changes in DNA solution viscosity [29]. The values of cube root of relative

specific viscosity $(\eta/\eta_0)^{1/3}$, where η is the viscosity of DNA in the presence of zinc oxide nanoparticle and η_0 , the viscosity of DNA alone were plotted against 1/R (R is equal to the ratio of the concentration of DNA to that of zinc oxide nanoparticle). Figure 10 shows the variation in the viscosity of DNA upon the addition of ZnO nanoparticles.

The addition of ZnO nanoparticles causes a slow increase in DNA viscosity in the regime of 1/R values ranging from 1 to 4 and decrease in the relative viscosity of DNA was observed for 1/R values between 4 and 5. Further addition of ZnO NPs causes a slight increase in relative viscosity. This behavior could be explained by any of the effects including the conformational changes, flexibility or the solvation of DNA molecules. But the most likely explanation is slightly lengthening of the DNA duplex. Since the ZnO and functionalized ZnO particles are electrostatically and independently moving molecules in the solution, this drags the viscosity winning that comes from molecules diffusing into each other. In our system, we can expect the partial intercalation of the ZnO nanoparticles between the base pairs of DNA. The overall behavior could be correlated to the toggling nature of ZnO NPs in binding with DNA between groove binding and electrostatic binding. A similar behavior in the viscosity of DNA were already been reported by Sathyanarayana et al. and by Dattagupta et al [30-32].

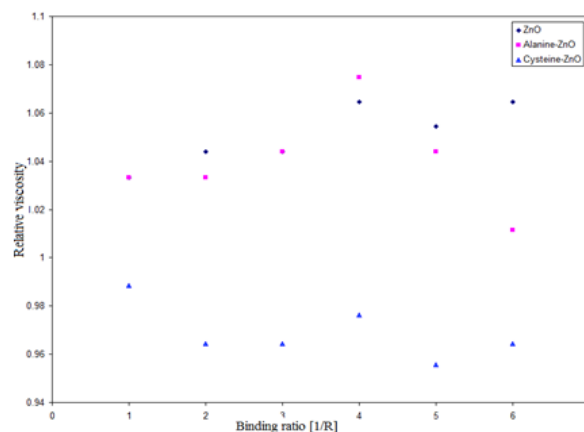


Fig 10:- Plot of relative viscosity of DNA Vs binding ratio for the ZnO as well as functionalized ZnO NPs.

IV. CONCLUSION

It is concluded that zinc oxide nanoparticles (ZnO NPs) in the range of 60-70 nm and the amino acid functionalized ZnO NPs are in the size of 80 nm with wurtzite phase. The bio active ZnO NPs and functionalized NPs might useful in the drug delivery. In this connection, we studied the ZnO NPs and functionalized ZnO NPs were interact with DNA through spectral investigation. We found the binding constant (K_b) assessed by UV-vis studies ($1.307 \times 10^5 \text{ M}^{-1}$, $2.531 \times 10^4 \text{ M}^{-1}$ and $4.23 \times 10^4 \text{ M}^{-1}$) indicate that there is a finite interaction between the NPs and DNA. From these K_b values, it may be clinched that the interaction may be feeble. The CD, DPV and viscosity measurements were corollary that the ZnO NPs interacted with DNA via electrostatic interaction or groove binding.

ACKNOWLEDGMENT

We thankfully acknowledge the Prof. PR. Athappan, Prof. & Head (Retd.,) Department of Inorganic Chemistry, School of Chemistry, for helpful discussion and guidance to complete the work as peaceful. We thank all the faculty members of Department of Inorganic Chemistry, School of Chemistry, for their help in UV-Vis and FT-IR spectra. Further, we thank the central instrumentation facility, Cochin University of Science and Technology (CUSAT) and Pondicherry University for their help in recording SEM-EDAX and XRD for throughout this work.

REFERENCES

- [1]. Kołodziejczak-Radzimska, A.; Jesionowski, T.; *Materials* **2014**, *7*, 2833–2881.
- [2]. Attarad, A.; Abdul-Rehman, P.; Zia, M.; *Nanotechnol. Rev.* **2018**, *7*(5), 413–441. <https://doi.org/10.1515/ntrev-2018-0067>.
- [3]. Zelechowska, K.; *BioTechnologia. J. Biotechnol. Comput. Biol. Bionanotechnol.* **2014**, *95*, 150–159.
- [4]. Sirelkhatim, A.; Mahmud, S.; Seeni, A.; Kaus, N. H.; Ann, L. C.; Bakhori, S. K.; Hasan, H.; Mohamad, D.; *Nano-Micro Lett.* **2015**, *7*, 219–242.
- [5]. Liu, J.; Feng, X.; Wei, L.; Chen, L.; Song, B.; Shao, L.; *Crit. Rev. Toxicol.* **2016**, *46*, 348–384.
- [6]. Cao, Y.; Gong, Y.; Liao, W.; Luo, Y.; Wu, C.; Wang, M.; Yang, Q.; *Bio Metals* **2018**, *31*, 457–476.
- [7]. Wingett, D.; Louka, P.; Anders, C. B.; Zhang, J.; Punnoose, A. A.; *Nanotechnol. Sci. Appl.* **2016**, *9*, 29–45.
- [8]. Khan, Y. A.; Singh, B. R.; Ullah, R.; Shoeb, M.; Naqvi, A. H.; Abidi, S. M.; *PloS One* **2015**, *10*, e0133086.
- [9]. Jiang, J.; Pi, J.; Cai, J.; *Bioinorg. Chem. Appl.* **2018**, <https://doi.org/10.1155/2018/1062562>.
- [10]. Yang, Y.; Zhang, C.; Hu, Z.; *Environ. Sci. Processes Impacts* **2013**, *15*, 39–48.
- [11]. Akhtar, M. J.; Ahamed, M.; Kumar, S.; Khan, M. A.; Ahmad, J.; Alrokayan, S. A.; *Int. J. Nanomed.* **2012**, *7*, 845–857.
- [12]. Rao, L.; Bu, L. L.; Cai, B.; Xu, J. H.; Li, A.; Zhang, W. F.; Sun, Z. J.; Guo, S. S.; Liu, W.; Wang, T. H.; Zhao, X. Z.; *Adv. Mater.* **2016**, *28*, 3460–3466.
- [13]. Biplab, K. C.; Paudel, S. N.; Rayamajhi, S.; Karna, D.; Adhikari, S.; Shrestha, B. G.; Bisht, G.; *Chem. Cent. J.* **2016**, *11*, 1734–1739.
- [14]. Cao, Y.; Xie, Y.; Liu, L.; Xiao, A.; Li, Y.; Zhang, C.; Fang, X.; Zhou, Y.; *Phytochem. Rev.* **2017**, *16*, 555–563.
- [15]. Zhang, C.; Mcadams, D. A.; Grunlan, J. C.; *Adv. Mater.* **2016**, *28*, 6292–6321.
- [16]. Ali, A.; Ambreen, S.; Javed, R.; Tabassum, S.; Ul Haq, I.; Zia, M.; *Mater. Sci. Eng. C.* **2017**, *74*, 137–145.
- [17]. Prabakaran, N.; Athappan, PR.; *J. Inorg. Biochem.* **2010**, *104*, 712–717.
- [18]. Prabakaran, N.; Murugesan, S.; Athappan, PR.; *J. Funct. Mater. Biomol.* **2018**, *2*, 40–47.
- [19]. Kalaimani, N.; Manivel, A.; Prabakaran, N.; *J. Funct. Mater. Biomol.* **2020**, *3*, 416–421.
- [20]. Wang, Z. L.; *J. Phys. Condens. Matter.* **2004**, *16*, R829–R858.
- [21]. Nandanatham, V.; Sampath Kumar, A. A.; Kathe, P. P.; Varatharajan, V.; *Nanotechnology* **2006**, *17*, 5087–5095.
- [22]. Zhang, Y.; Jin, Mu.; *Nanotechnology.* **2007**, *18*, 075606.
- [23]. Wu, Z. Y.; Chen, F.R.; Kai, J. J.; Jian, W. B.; Lin, J. J.; *Nanotechnology* **2006**, *17*, 5511–5518.
- [24]. Panigrahi, S.; Kundu, S.; Basu, S.; Praharaj, S.; Jana, S.; Pande, S.; Ghosh, S.K.; Anjali, P.; Tarasankar, P.; *Nanotechnology.* **2006**, *17*, 5461–5468.
- [25]. Kleinwechter, H.; Janzen, C.; Knipping, J.; Wiggers, H.; Roth, P. *J. Mater. Sci.*, **2002**, *37*, 4349–4360.
- [26]. Mandal, S.; Gole, A.; Lala, N.; Gonnade, R.; Ganvir, V.; Sastry, M.; *Langmuir* **2001**, *17*, 6262–6268.
- [27]. Aryal, S.; Remant, B. K. C.; Dharamraj, N.; Bhattarai, N.; Kimand, C. H.; Kim, H. Y.; *Spectrochim. Acta A.* **2006**, *63*, 160–163.
- [28]. Zsila, F.; Bikadi, Z.; Simonyi, M. *Org. Biomol. Chem.* **2004**, *2*, 2902–2910.
- [29]. Lerman, L.; *J. Mol. Biol.* **1961**, *3*, 775–779.
- [30]. Sathyanarayana, S.; Dabrowiak, J. C.; Chaires, J. B.; *Biochemistry.* **1993**, *32*, 2573–2584.
- [31]. Yang, G.; Wu, J.Z.; Wang, L.; Ji, L. N.; Tian, X.; *J. Inorg. Biochem.* **1997**, *66*, 141–144.
- [32]. Dattagupta, N.; Hogan, M.; Crothers, D. M.; *Proc. Natl. Acad. Sci., USA* **1978**, *75*, 4286–4290.